Wave-induced soil liquefaction

recent failure of a coastal buried pipeline and the applicability of known analytical models for the liquefaction risk assessment

Antonini, Alessandro; Lamberti, Alberto

Important note
To cite this publication, please use the final published version (if applicable).
Please check the document version above.

Wave-induced soil liquefaction: recent failure of a coastal buried pipeline and the applicability of known analytical models for the liquefaction risk assessment

Alessandro Antonini
Department of Hydraulic Engineering, Delft University of Technology, Delft, The Netherlands
Alberto Lamberti
Department of Civil, Chemical, Environmental and Material Engineering, University of Bologna, Bologna, Italy

ABSTRACT

The recent failure of a coastal buried pipeline along the Italian coast is presented. Extensive initial investigations to assess failure causes are conducted and several shreds of evidence are identified leading to wave-induced liquefaction as the main source of failure. This thesis is subsequently confirmed through the application of two known analytical models, i.e. Ishihara and Yamazaki 1984 and Sumer et al., 2012. The results show that despite the rather inexpensive computational cost of the models, they can be successfully used to identify the area affected by the wave-induced liquefaction with good agreement with field observation.

KEY WORDS: Wave induced soil liquefaction; Coastal buried pipelines

INTRODUCTION

Wave-induced instability of seabed soils around buried pipelines is an increasingly important research subject concerning the stability of pipelines transporting hydrocarbons from wells to processing facilities (Pisanò et al., 2022), of pipelines for outflow discharge and of cable connections for marine renewable energy. When directly laid on the seabed, pipelines are often exposed to harsh hydrodynamic loads or collisions with hard bodies that may negatively impact their structural performance. A typical stabilization option is to lay pipelines in trenches backfilled with rocks or sand. Since sand backfills are often loose (uncompacted) and shallow (i.e. subject to low effective compression), Pipelines buried in sandy backfill may suffer from the consequences of soil liquefaction because they can move in liquefied sands (Pisanò et al., 2020). Liquefaction can be triggered by a number of factors, including structural vibrations, ocean waves, and earthquakes (Sumer, 2006). The occurrence of liquefaction is generally associated with low values of relative density of the backfill in combination with low effective stresses at shallow soil depth, however, influence of the previous stress/strain history can also play a role (Nelson and Okamura, 2019). Liquefied soils are characterized by low strength and stiffness inducing segments of buried pipelines to experience excessive displacement, for instance in the form of vertical flotation or sinking. In the presence of either relatively light or heavy pipelines, the difference between the pipeline and the liquefied sand weight is the main trigger of the flotation or sinking process. The process of buried pipelines flotation is well known since 1966 with the study conducted within the Pipeline Floatation Research Council framework in US (Pipeline Flotation Research Council, 1966),

while later additional studies and documented pipeline failures were reported by Christian et al. (1974), Herbich et al. (1984) and Damgaard et al. (2006). EU wise, considerable research effort was invested on the wave induced liquefaction problem through the LIMAS project ended in 2004, (Damgaard et al., 2006; Sumer, 2006; Sumer, 2014; Sumer et al., 2010; Sumer et al., 2006; Sumer, 2012) while more recently the ongoing NuLIMAS project is developing open source numerical tools to model the liquefaction around marine structures, (Shanmugasundaram et al., 2022; Sumer and Kirca, 2022). Some relevant outcomes of the previous research efforts are reflected within some industry standards, however, it is the opinion of this paper's authors that no specific methodologies are explicitly mentioned to assess the risk of wave induced liquefaction. Indeed, industry practice relies on the designer experience who rather often assumes liquefaction around buried pipelines as a given fact, whose negative effects can be mitigated by designing heavier pipelines and rock protection. The twofold goal of this work is to present a recent case of coastal buried pipeline failure due to wave induced liquefaction and to highlight the predictive capability of simple and computationally inexpensive models such as Ishihara and Sumer's models (Ishihara and Yamazaki, 1984; Sumer, 2012). The effectiveness of the models will be quantified by contrasting their prediction in terms of liquefied trench area and the observed pipelines failure.

CASE STUDY

Case study description

Within the activities framework aimed to improve the beach and sea conditions in front of Rimini (Emilia-Romagna region, Italy) three submarine pipelines were built to release around 1 km offshore the Ausa torrent discharge during extreme events, Fig. 1.a. The entire system was built between 2017 and 2020 while the marine works only started in 2019. The three 2.0 m inner diameter and 36 mm thick fiberglass (density γc=1850 kg/m^3) pipelines extend from inshore - where the hydraulic head is guaranteed by a water tower - to offshore, perpendicularly to the coastline, i.e. 55° north, Fig. 1.b. The pipelines' release point is set at 7.2 m water depth. Each pipeline is made of 12 m long elements connected to each other through a spigot-socket joint. The three pipelines were installed in a common trench, 4.1 m deep below the seabed, and dug into the sandy bottom (dry weight γ_s=1800 kg/m^3) aimed to guarantee protection from the hydrodynamic loads and accidental anchor impacts.

Fig. 1 a) Case study location overview, b) Satellite image during the construction of the pipelines in June 2020 and work area localization, from Google Earth.

The trench was realized with two different methodologies. For the first 270 m near the shoreline it is bounded by sheet piles with a variable width that reaches the maximum value of 25 m at its end around 2.75 m water depth (offshore limit). The remaining part of the trench is 10 m wider and is dug into the sandy bottom without lateral containment or support, Fig. 2. The sandy cover above the pipeline ranges between 1.7 and 2.0 m and was realized with the bottom material previously removed to excavate the trench. Backfilling is realized through two different methods: the first part, bounded by sheet piles, is backfilled through sequential sandy layers placed by a crane, while the remaining part of the trench (i.e. the most offshore one) is backfilled by loose sand positioned by a crane operating on a floating barge without any layer consideration. Both backfilling operations did not account for any compaction check or limit, e.g. achieved relative density. 1+1 m³ saddlebags filled with sand are positioned above each pipeline on average every 4 m to increase the stability of the pipelines, however, the contact between pipeline and saddlebags has not been guaranteed by any mechanical means.
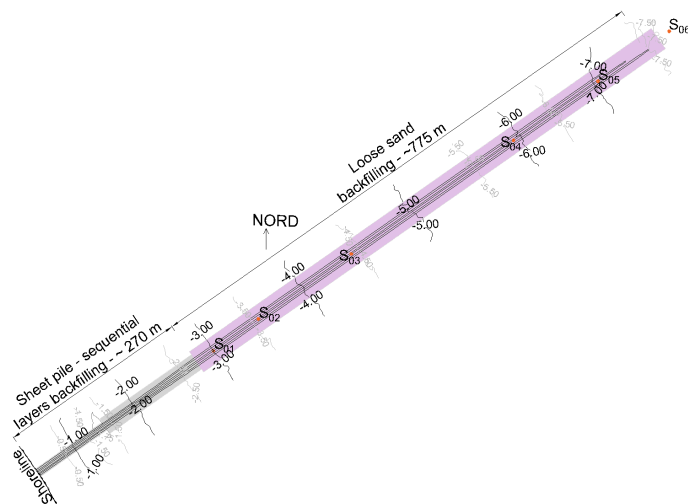

Fig. 2 Plan view of the pipeline marine part, bathymetry, trench parts distinction and location of the geotechnical surveys (S$_{01}$-S$_{06}$ along the open trench). Grey filling identifies sheet pile bounded trench and backfilled via layers, purple filling open trench no layers backfilling.

Between January 2019 and February 2021, 14 minor north-eastern storms (i.e. significant wave height (H$_S$) between 2.0 and 3.6 m) affected the pipelines location with maximum H$_S$ value equal to 3.6 m.

In April 2021, during the pumps-pipelines system test, the first signs of pipeline failures appeared in the form of a darker water whiff at the sea surface. Later, as a result of a multibeam and divers surveys, the emergence failure of the pipelines was confirmed. The southernmost pipeline lifted around 3.0 m and emerged from the bottom around 650 m from the shoreline at 5.0 m water depth while a rather large cavity was created shoreward, Fig. 3; the northernmost pipeline lifted 1.5 m from its original position around 450 m from the shoreline between 3.9 and 4.5 m water depth.
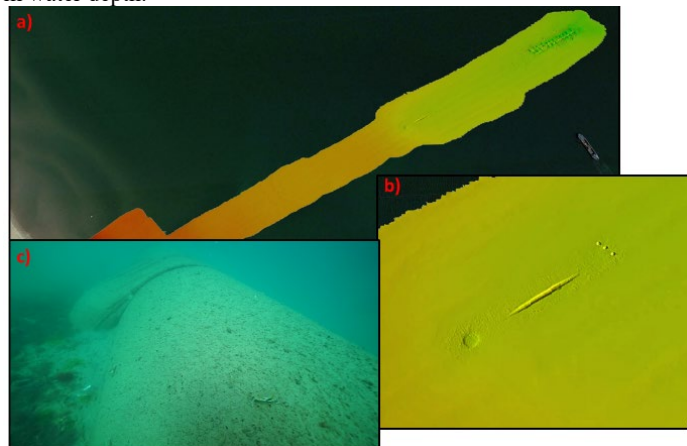
Fig. 3 a-b) Multibeam survey and c) under water picture highlighting the southernmost pipeline and the three manholes emersion and the shoreward cavity.

Wave data

Wave data such as significant wave height (H$_S$), peak period (T$_P$) and mean wave direction (Alpha) are available at the Nausicaa wave buoy installed 20 km north-west the interested area, i.e. off the city of Cesenatico on 10 m water depth, Fig. 4. The data are acquired every 30 minutes and covers the entire period between 1st January 2019 and 28th February 2021.

Fig. 4 Nausicaa wave buoy location

The bathymetry between the wave buoy and off the pipeline location is rather constant without considerable variations, therefore the records can be considered a reasonable source of information to describe the wave climate offshore the interested ar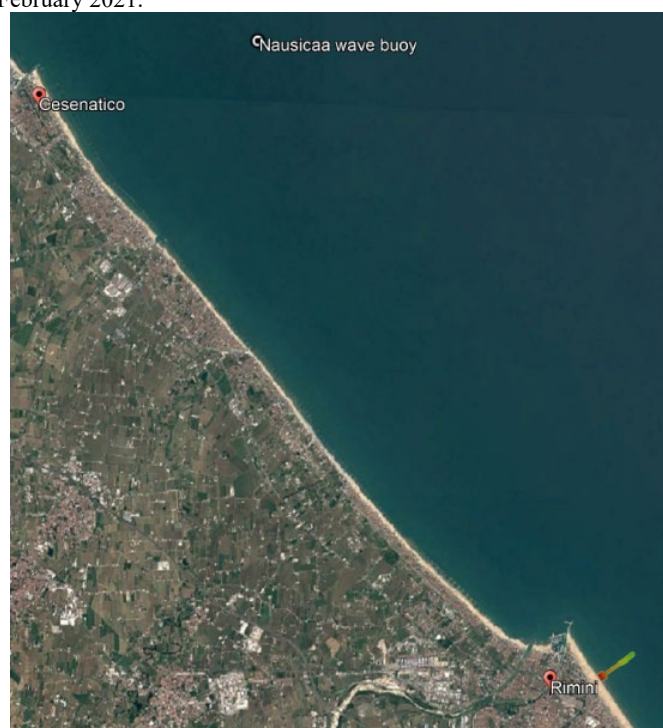ea. The analysis on the wave data is aimed at identifying bulk parameters (i.e. H_S, T_P and Alpha) that can be used to describe an average storm condition occurred during the investigated time interval. Therefore, not only the peaks associated with each storm event are selected, but the entire part of the time series above the thresholds is considered to extract average values. The threshold is set to 2.5m H_S, identifying 12 storms and overall 89 measurements that are considered sufficient to have good description of the average event Fig. 5.
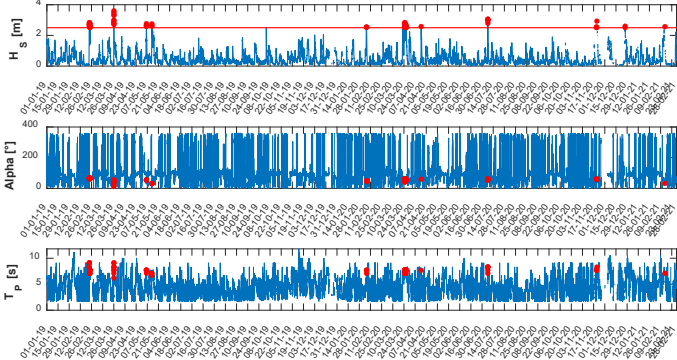
Fig. 5 Wave data from 1st January 2019 to 28 February 2021.

By clustering the data according to the two thresholds, clearly appears that the characteristics of the storms are rather similar. All the storms are mainly generated by the north-westerly Bora wind with a dominant direction between 60 and 40° N, Fig. 6. The average parameters are presented in Table 1.
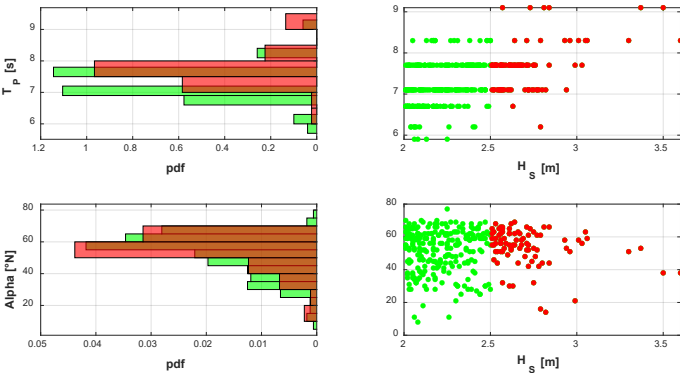
Fig. 6 H_S, T_P and Alpha distribution.

Table 1 Average sea state parameters – 10 m water depth

	Threshold 2.5 m		
	H_S [m]	T_P [s]	Alpha [°]
Mean	2.71	7.7	54
Median	2.64	7.7	56
std	0.21	0.6	11

The values presented in Table 1 are representative of the offshore condition at 10 m water depth. The average direction is equal to 54° N, by chance, the same as the alignment of the pipeline, therefore, by neglecting the minor refraction effects, the waves act along the pipeline's development inducing small to no lateral actions on the emerged or uncovered pipelines. Furthermore, under these conditions the main processes affecting the wave propagation are only shoaling and wave breaking that can be properly captured by phase-averaged models

(Antonini et al., 2017) through a simple one-dimensional SWAN model (Booij et al., 1999), while H_{rms} and median wave height (H_m) are quantified by the composite Weibull distribution proposed by Battjes and Groenendijk (2000), Fig. 7.
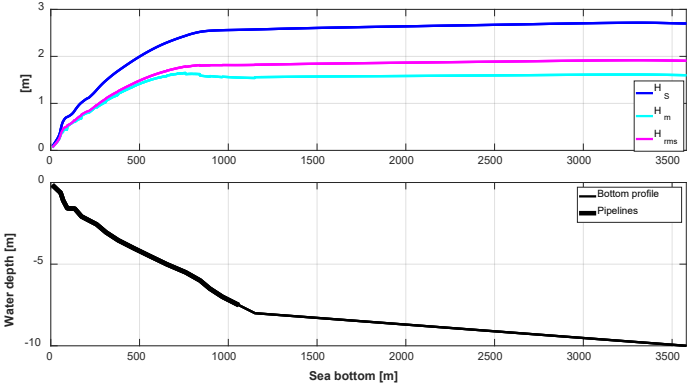
Fig. 7 H_S, H_{rms} and H_m propagation along the pipelines profile according to the average sea state presented in Table 1.

Geotechnical & Geological data

Prior to the realization of the pipelines system, i.e. spring 2017, vibro-core investigation has been performed to characterize the bottom material stratigraphy below the pipeline installation area. 6 locations (hereafter called S_{01}-S_{06}, Fig. 2) along the pipelines developments have been targeted to extract 4 samples of material for each location through the vibro-core equipment. The water depth corresponding to the samples' area spans from 3 to 8.5 m, while the maximum depth of the sample was around 5 m below the mud line. The nearshore bottom is mainly composed of fine quartz sand ($S_{01,2}$) while moving more offshore, after 4.5 m water depth, deep clay and clayey silt layers bound the top sand layer while following the natural slope of the bottom, Fig. 8.
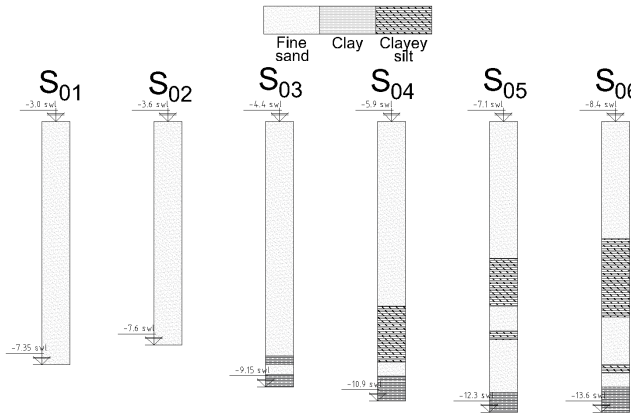
Fig. 8 Samples collected along the pipeline area.

The average parameters characterizing the sandy layer are: dry unit weight (γ_s) 1920 kg/m³, units weight of solids (γ_{ss}) 2650kg/m³, content of fine, i.e. clay and silt, (FC) 15%, D_5 0.015mm, D_{10} 0.045mm, D_{50} 0.095mm, D_{60} 0.11mm. Hence the coefficient of uniformity (C_U) is 2.4 and the void ratio (e) 0.8. The specific weight of sea water (γ_{ws}) is assumed equal to 1020 kg/m³. The remaining geotechnical parameters required for the application of Ishihara and Sumer's model such as, minimum and maximum void ratio (e_{min} and e_{max}), porosity (n), bulk modulus of elasticity of water assuming saturated soil (K), permeability (k), friction angle (φ) young modulus (E), shear modulus (G), Poisson modulus (v) and consolidation coeff. (c_v) are estimated through empirical formulas available in literature and provided in Table 2.

Table 2 Estimated geotechnical parameters

Variable	Value	Equation	Reference
D_r	30-45	$\dfrac{e_{max} - e}{e_{max} - e_{min}}$	Lambe and Whitman (1969); van 't Hoff and van der Kolff (2012)
e	0.89-0.81	N.A.	Field samples
e_{min}	0.5	N.A.	Cubrinovski and Ishihara (2002); Lambe and Whitman (1969);Sumer (2006)
e_{max}	1.06	$0.43+0.00867 \cdot FC + e_{min}$	Cubrinovski and Ishihara (2002)
k	0.0074 – 0.0076 cm/s	$2.4622 \left(\dfrac{d_{10}^2 \cdot e^3}{1+e} \right)^{0.7825}$	Chapuis (2004)
n	0.44 - 0.45	$\dfrac{e}{1+e}$	Lambe and Whitman (1969)
K	$1.9 \cdot 10^6$ kN/m²	N.A.	Sumer (2014)
φ	34-34.2°	$28+0.14 \cdot D_r$	Schmertmann (1978)
E	18160 kN/m²	N.A.	Lambe and Whitman (1969); Look (2014); Sumer (2014)
υ	0.20-0.25	N.A.	Look (2014) Sumer (2014)
G	7560-10880 kN/m²	$\dfrac{E}{2 \cdot (1+\upsilon)}$	Sumer (2014)
c_v	0.181-0.238 m²/s	$\dfrac{G \cdot k}{\gamma_{ws}} \cdot \dfrac{2-2 \cdot \upsilon}{(1-2 \cdot \upsilon)+(2+2 \cdot \upsilon) \cdot \frac{n \cdot G}{K}}$	Sumer (2014)

METHOD

Several computationally expensive models are available to model wave-induced liquefaction, e.g. CFD and FEM (e.g. Sassa and Sekiguchi (2001); Shanmugasundaram et al. (2022)), however their applicability is limited by the required computational time. On the other hand, the analytical Ishihara's model (Ishihara and Yamazaki, 1984) and Sumer's model (Sumer, 2014; Sumer, 2012) are computationally inexpensive and thus suitable for the liquefaction risk assessment under large uncertainty. Ishihara's model is the first analytical model developed to investigate the risk of wave induced liquefaction of a sandy sea bottom based on the offshore wave conditions. The model assumes a regular wave train characterized by offshore wave conditions H_0 and L_0 (no more specific reference is provided to select the wave height, e.g. H_s, H_m, H_1, etc…) that propagates on a slopping bottom profile. The sandy bottom is assumed to be an elastic semi-space bounded by the seabed while unlimited along the negative vertical direction. The soil's mechanical properties are constant and isotropic. The differential cyclic load induced by the waves generates shear stress within the soil body that in turn can exceed the critical value, only function of the relative density (D_r), and therefore produces large deformations or liquefaction of the sandy body. Therefore, the model only r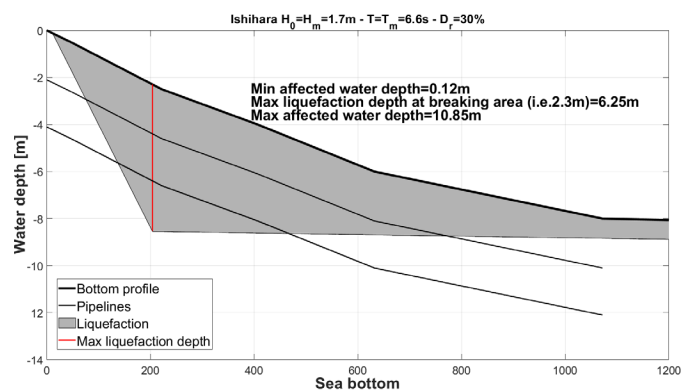equires offshore wave conditions and relative density. The full description of the model can be accessed from the original Ishihara's work, Ishihara and Yamazaki (1984)

Sumer's model describes the time and space (along the vertical direction) build-up of pore pressure due to the propagation of a regular wave train. The mechanical soil properties are homogenous within the sandy layer while the model allows to account for a deeper impermeable boundary that does not allow pore pressure propagation and dissipation. The hydrodynamic forcing is due to the local wave conditions (while for Ishihara's model the offshore wave conditions are required), for which it is suggested to conservatively assume the local value of H_{rms} and T_z. Therefore, the model aims to capture the conditions for the initiation of the liquefaction process governed by the ratio between the accumulated pore pressure and the initial mean normal effective stress within the soil column. When this ratio is larger than one liquefaction occurs. The complete description and validation of Sumer's model are presented in Sumer (2014); Sumer (2012).

RESULTS

Ishihara's model

Fig. 9 shows the results of Ishihara's model for 4 tested conditions. Two D_r values have been adopted. D_r equal to 30% is related to sand dumped under water as the case of the trench filling material (van 't Hoff and van der Kolff, 2012), while 45% is defined according to the sampled field material for undistrubed conditions, i.e. samples exposed to waves action, therefore likely to be denser than the material used to fill the trench. Moreover, both combinations of hydrodynamic forcing parameters, i.e. H_m-T_m and H_{rms}-T_z, have been used to assess the sensitivity of the model to different wave parameters. The results highlight the non-negligible risk of liquefaction for all conditions in the pipelines area. D_r plays a fundamental role in the extension of the liquefiable area that extends from around the shoreline to offshore for D_r equal to 30% while remaining limited within the area of the pipelines for 45%. In both cases the maximum liquefaction penetration reaches the bottom of the trench. The tested wave parameters play a minor role, however, the effect of a longer period is reflected in larger liquefied areas, while higher wave heights have the main effect of pushing the maximum liquefaction point slightly more offshore and increasing its magnitude. The results for D_r equal to 30% show rather good agreement with the observed damages as a large part of the pipelines are embedded in liquefied soil between 400 and 600 m from the shoreline, whereas the results for higher D_r value, still highlight serious threat from the liquefaction phenomena, but do not perfectly match the damaged area. Overall the adopted model is based on several simplifications for the description of the soil behavior (the soil is completely characterized through its weight and relative density), however, this is not only a limit but, perhaps, also its strength due to the reduced number of parameters that must be known or estimated to obtain preliminary results.
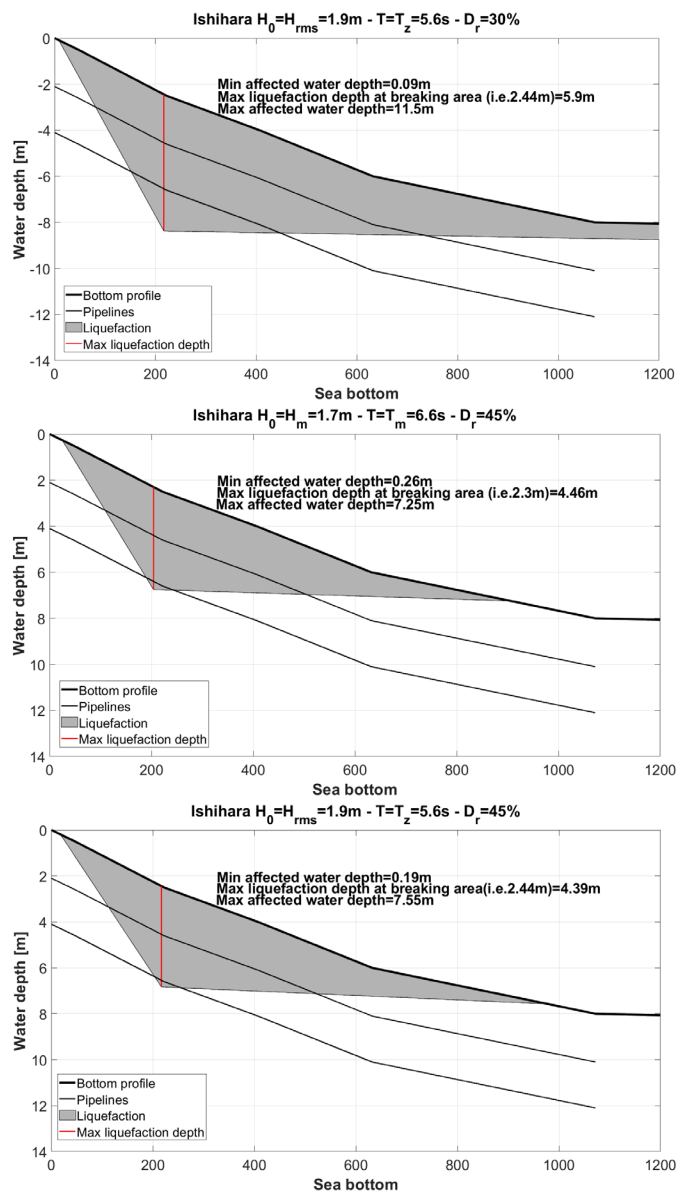

Ishihara $H_0=H_m=1.7m$ - $T=T_m=6.6s$ - $D_r=30\%$

Min affected water depth=0.12m
Max liquefaction depth at breaking area (i.e.2.3m)=6.25m
Max affected water depth=10.85m

Fig. 9 Ishihara model results. First panel D_r=30% H_m-T_m, second panel D_r=30% H_{rms}-T_z, third panel D_r=45% H_m-T_m, fourth panel D_r=45% H_{rms}-T_z

Sumer's model

Fig. 10 shows the results of Sumer's model for two tested conditions. The figure is divided into two parts. In the top part the local wave height, either H_m or H_{rms}, is presented with a blue line as the result of the SWAN model and the application of Battjes and Groenendijk (2000) distribution for depth limited individual wave height. Only the results for D_r equal to 30% are proposed because the model does not highlight any risk of liquefaction for D_r equal to 45%. However, this disagreement between the two models is mainly due to the large number of geotechnical parameters that had to be estimated from empirical formulas. Indeed, the use of Sumer's model requires all the parameters proposed in Table 2 as input, making it highly sensitive to the underlying uncertainties. Despite this, the proposed results for D_r equal to 30% present a remarkable good agreement with the observed damages. Both the combinations of wave parameters, properly capture the area of the observed pipelines' failure between 400 and 650 m from the shoreline. The liquefaction reaches the bottom of the trench in both cases, however, the extension of the

liquefied area is rather sensitive to the adopted wave parameters. The discrepancy appears also in terms of limits of the liquefied area as Sumer's model, coupled with the complete description of the local wave heights, clearly concentrate the liquefied area around the breaking region detected through the hydrodynamic simulation. The liquefaction does not extend too offshore as for Ishihara's model, and the affected maximum water depth is 6.4 and 7.6 m for H_m-T_m and H_{rms}-T_z respectively. The agreement with the observed damages is rather good clearly pointing out that liquefaction might have been the source of the pipelines' failure. Despite Sumer (2014) empirical evidence clearly indicates the use of the combination H_{rms}-T_z to describe the irregular wave field, in this work we propose the use of two different sets of wave parameters, namely H_m-T_m and H_{rms}-T_z, because, in our view, it remains an open question whether the liquefaction is a process related to an energetic similarity between the irregular waves field and the corresponding regular one, i.e. adopting H_{rms}-T_z, or whether the liquefaction is related to the mean process, i.e. adopting H_m-T_m.
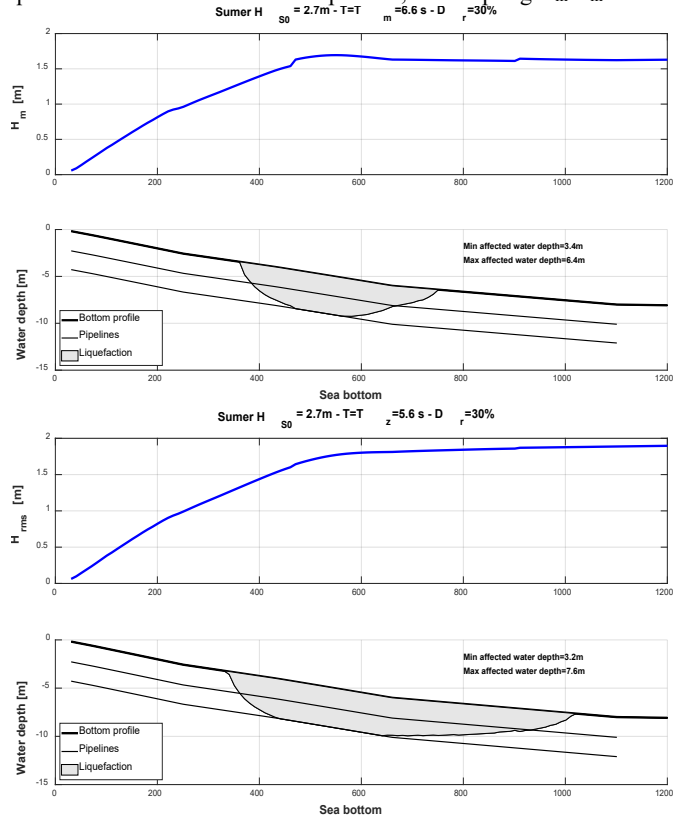

Fig. 10 Sumer model results. Upper panel D_r=30% H_m-T_m, lower panel D_r=30% H_{rms}-T_z

DISCUSSION

From the proposed analysis, it is evident that liquefaction might have happened at the investigated location. However, no direct measurements were available to confirm it. On the other hand, damages due to liquefaction were observed. The rather light pipeline floatation is particularly evident where the models' results highlight that the liquefied sandy layer reaches the trench bottom. Flotation did not happen everywhere: the relative density of the backfilling material was not controlled during the realization, generating large spatial variability, while at the same time, the adopted models show really high sensitivity to its value. Finally, being the investigated location close to a river mouth, the spatial (both planar and vertical) variability of the material might have induced different responses along the development of the pipelines.

CONCLUSIONS

This work presents a recent coastal buried pipelines failure and the investigation carried out to identify the underlying reasons. Several shreds of evidence were collected, among others wave conditions before the observation of the failure, the type of soil and multiple bathymetric surveys. Wave induced liquefaction appeared as the most plausible phenomenon that led to the failure. To corroborate this hypothesis two known models were adopted combining the few data available. Both Ishihara (Ishihara and Yamazaki, 1984) and Sumer's (Sumer, 2012) model confirm that the liquefaction could be the cause of the detected movement of the pipelines. Different wave parameters and relative density values were tested with both models obtaining similar results concerning the wave parameters, whereas different relative density values and the underlying dependencies with the geotechnical parameters produced different results according to the adopted model. However, both models confirm that for a relative density equal to 30% wave induced liquefaction could be the cause of the failure. In order to refine the investigation a thorough geotechnical field campaign should be carried out to provide the required parameters and reduce the uncertainties due to the adopted empirical formulas.

REFERENCES

Antonini, A., Archetti, R. and Lamberti, A., 2017. Wave simulation for the design of an innovative quay wall: The case of Vlorë harbour. Nat. Hazards Earth Syst. Sci., 17(1): 127-142.

Battjes, J.A. and Groenendijk, H.W., 2000. Wave height distributions on shallow foreshores. Coastal Engineering, 40(3): 161-182.

Booij, N., Ris, R.C. and Holthuijsen, L.H., 1999. A third-generation wave model for coastal regions: 1. Model description and validation. Journal of Geophysical Research: Oceans, 104(C4): 7649-7666.

Chapuis, R.P., 2004. Predicting the saturated hydraulic conductivity of sand and gravel using effective diameter and void ratio. Canadian Geotechnical Journal, 41(5): 787-795.

Christian, J.T., Taylor, P.K., Yen, J.K.C. and Erali, D.R., 1974. Large diameter underwater pipeline for nuclear power plant designed against soil liquefaction. Offshore technology conference, p.^pp.

Cubrinovski, M. and Ishihara, K., 2002. Maximum and minimum void ratio characteristics of sands. Soils and Foundations, 42(6): 65-78.

Damgaard, J.S. et al., 2006. Guidelines for pipeline on-bottom stability on liquefied noncohesive seabeds. Journal of Waterway, Port, Coastal, and Ocean Engineering, 132(4): 300-309.

Herbich, J.B., Schiller, R.E., Dunlap, W.A. and Watanabe, R.K., 1984. Design guidelines for ocean-founded structures. Marcel Dekker Inc.

Ishihara, K. and Yamazaki, A., 1984. Analysis of wave-induced liquefaction in seabed deposits of sand. Soils and Foundations, 24(3): 85-100.

Lambe, T.W. and Whitman, R.V., 1969. Soil mechanics. Technology & engineering. John Wiley & Sons.

Look, B.G., 2014. Handbook of geotechnical investigation and design tables. Taylor & Francis Group.

Nelson, F. and Okamura, M., 2019. Influence of strain histories on liquefaction resistance of sand. Soils and Foundations, 59(5): 1481-1495.

Pipeline Flotation Research Council, 1966. Asce preliminary research on pipeline flotation. Journal of the Pipeline Division, 92(1): 27-74.

Pisanò, F., Betto, D., Della Vecchia, G. and Cremonesi, M., 2022. Pipeline flotation in liquefied sand: A simplified transient model. Ocean Engineering, 266.

Pisanò, F., Cremonesi, M., Cecinato, F. and Della Vecchia, G., 2020. Cfd-based framework for analysis of soil–pipeline interaction in reconsolidating liquefied sand. Journal of Engineering Mechanics, 146(10).

Sassa, S. and Sekiguchi, H., 2001. Analysis of wave-induced liquefaction of sand beds. Géotechnique, 51(2): 115-126.

Schmertmann, J.H., 1978. Guidelines for cone penetration test (performance and design), U.S. Department of Transportation.

Shanmugasundaram, R.k. et al., 2022. Towards the numerical modelling of residual seabed liquefaction using openfoam. OpenFOAM® Journal, 2: 94-115.

Sumer, B.M., 2006. Liquefaction around marine structures. Processes and benchmark cases. ASCE Journal of Waterway, Port, Coastal and Ocean Engineering, 132(4): 225-335.

Sumer, B.M., 2014. Liquefaction around marine structures. Advance series on ocean engineering, 39. World Scientific Publishing Co. Pte. Ltd.

Sumer, B.M., Figen, H.D. and Jørgen, F., 2010. Cover stones on liquefiable soil bed under waves. Coastal Engineering, 57(9): 864-873.

Sumer, B.M., Figen, H.D., JØRgen, F. and Sumer, S.K., 2006. The sequence of sediment behaviour during wave-induced liquefaction. Sedimentology, 53(3): 611-629.

Sumer, B.M. and Kirca, V.S.O., 2022. Scour and liquefaction issues for anchors and other subsea structures in floating offshore wind farms: A review. Water Science and Engineering, 15(1): 3-14.

Sumer, B.M., Ozgur Kirca, V.S.O., Fredoe, J., 2012. Experimental validation of a mathematical model for seabed liquefaction under waves. Journal of Offshore and Polar Engineering, 22(2): 133-141.

van 't Hoff, J. and van der Kolff, A.N., 2012. Hydraulic fill manual, Ciria, Boca Raton, London, New York, Leiden.